Proceedings World Geothermal Congress 2026
Calgary, Canada, June 8 – 11, 2026

Rapid Source Parameters Estimation of Earthquakes in Geothermal Field by the Back-Projection Method

Bor-Shouh Huang[1]*, Hsin-Hua Huang[1], Chung-Hsiang Mu[1], Chin-Shang Ku[1], Chin-Jen Lin[1], Sheng-Rong Song[2], Jian-Cheng Lee[1]

Institute of Earth Sciences, Academia Sinica, Taipei, Taiwan[1], Department of Geosciences National Taiwan University, Taipei, Taiwan[2]

E-mail address: hwbs@earth.sinica.edu.tw

Keywords: geothermal field, seismic array, back projection, optimization design

INTRODUCTION

The massive use of fossil fuels by humans has led to substantial carbon dioxide emissions into the atmosphere, driving the greenhouse effect, global warming, and climate change—threatening the survival of humans, animals, and plants. To reduce reliance on fossil fuels, scientists have proposed the use of green and sustainable alternative energy sources, alongside the development of carbon capture and storage technologies, aiming to cut CO_2 emissions and slow global warming. Among these solutions, geothermal energy development and geological CO_2 storage are considered particularly effective. Enhanced Geothermal Systems (EGS), which improve geothermal energy efficiency, and Carbon Capture and Storage (CCS), which enables large-scale sequestration, have both been introduced and are in early testing phases. These technologies rely on modifying subsurface geological conditions to create favorable environments. However, because such changes affect the Earth's internal stress state, they may, under certain circumstances, induce earthquakes. Indeed, seismic events have been reported in existing geothermal experiments and development projects.

In fact, during both the development testing and operational phases, all geothermal sites may be impacted by significant nearby natural earthquakes, as well as by induced earthquakes caused by water injection during power plant testing and operations. These risks emphasize the need for a robust seismic monitoring and reporting system in geothermal areas to track stress changes around the site, ensure effective operational management, and minimize disaster risks.

In Taiwan, we have experienced to use dense seismic network data to study the source characteristics and wave propagation of large earthquakes, as well as to support rapid reporting and earthquake early warning. These efforts have established experience in applying seismic array techniques to natural earthquake research.

In this study, we aim to adapt and apply regional array techniques, originally used for natural earthquake studies, to small-scale investigations in geothermal areas. By arranging waveforms from seismic array and employing stacking imaging process, this research seeks to identify the locations of induced earthquakes in geothermal fields by the back-projection method and determine their source mechanisms by arrangement stacking of the first polarity.

METHODS

In this study, we present an automated method for processing data from a dense strong-motion network. Using a back-projection (BP) approach, we determine the hypocenter location of an earthquake and estimate its focal mechanism by waveform stacking. We hope to develop a new algorithm capable of event relocation and focal mechanism determination over a wide magnitude range.

1. The relocation of event relies on the superposition of seismic wave energy, instead of relying on arrival time information for location analysis. It back-projects the seismic wave amplitude to the source location based on the wave propagation path (or travel time on seismic trace). Notably, it does not require picking arrival times; instead, it utilizes a search procedure to repeatedly migrate and superimpose seismic wave energy to identify the optimal epicenter location. This method requires array waveform data recorded by stations distributed around the source. The analysis process involves grid searching, treating all grid points within the model as potential source locations, and calculating the travel time difference from each grid point to all stations using an appropriate velocity model, e.g., Ishii et al. (2007). By shifting the recorded seismograms of each station based on the calculated travel time for all grid points in the model, the seismic wave energy is stacked to obtain

corresponding peak values. The grid point with the maximum peak value is considered as the true source, and its corresponding time is the origin time. The key calculation steps can be represented by the following formula:

$$\mathrm{Stack}_i(t) = \frac{1}{N}\sum_{k=1}^{N} S_k\,(t - t_{ik}) \tag{1}$$

where $\mathrm{Stack}_i(t)$ is the time series of the total stacked seismic waveforms, *N* is the number of stations, *k* is the station number, $S_k(t)$ is the seismic amplitude time series of the kth station, and t_{ik} is the theoretical travel time calculated from grid point *i* in the model to the station *k*, e.g., Ishii et al. (2007).

2. The method employed in this study to infer the seismic source mechanism through analysis of seismic wave polarities is described as follows:

$$\boldsymbol{S}(\emptyset, \delta, \lambda) = \sum_{k=1}^{n} sgn[P_k\,(\emptyset, \delta, \lambda, \emptyset_s, i_\xi)] * UD_k(\emptyset_s, i_\xi) \tag{2}$$

where,

$$P_k(\emptyset, \delta, \lambda, \emptyset_s, i_\xi) = cos\lambda\ sin\delta\ sin^2 i_\xi sin2(\emptyset - \emptyset_s) - cos\lambda\ cos\delta sin2i_\xi\ cos(\emptyset - \emptyset_s) + sin\lambda\ sin2\delta(cos^2 i_\xi - sin^2 i_\xi sin^2(\emptyset - \emptyset_s) + sin\lambda\ cos2\delta\ sin2i_\xi\ sin(\emptyset - \emptyset_s)$$

In this formula, $P_k(\emptyset, \delta, \lambda, \emptyset_s, i_\xi)$ represents the theoretical P-wave amplitude estimated for the k-th seismic station using a theoretical radiation pattern. $\emptyset_s$ and i_ξ respectively represent the azimuth and ray exit angle of the seismic station relative to the source. The theoretical P-wave radiation pattern $P_k(\emptyset, \delta, \lambda)$, represents with the source parameters of azimuth angle ∅, dip angle δ, and slip angle λ, respectively, e.g., Aki and Richards (2002). *sgn* is the signum function determines the sign of a number. UD_k denotes the vertical component polarity of the k-th seismic record (upward for 1 and downward for -1). The stacking variable S represents the result of calculating the right side of Equation (2) for all records (n seismic stations). The analysis will use previously extracted P-wave polarity data as input (upward for 1 and downward for -1) and assign the data weight based on its polarity computed from theoretical radiation pattern (up for 1 and down for -1). This stacking process will search for grid points of fault strike, dip and slip parameters. By examining all possible parameter values and ultimately evaluating them through stacked extremities.

According to the calculation in Equation (2), determining the focal mechanism requires first identifying the P-wave polarity at each recording station, and then inferring the focal mechanism solution from the picked polarities of seismic phases arriving at the stations. To pursue a more direct method for focal mechanism determination. Thus, it does not require pre-picking P-wave polarities at each station but directly stack the recorded waveforms from the stations to infer the focal mechanism. In this study we attempt to generalize S in Equation (2) to Equation (3),

$$S(\phi, \delta, \lambda, x_0, y_0, z_0, t_0) = \sum_{k=1}^{n} sgn[P_k(\phi, \delta, \lambda, \phi_s, i_\xi)] * T_k(\phi_s, i_\xi, x_0, y_0, z_0, t_0) \tag{3}$$

Compared with Equation (2), T_k in Equation (3) is generalized to the seismogram aligned using the corrected source location and origin time (x_0, y_0, z_0, t_0) obtained from BP estimation, i.e., the waveforms after applying time shifts corresponding to that source position and time. The variable S of Equation (3) represents the stacked signal of the corrected seismic records and is a time-series seismogram. The optimal focal mechanism under this generalization is still found by grid searching the parameter space of strike ϕ, dip δ, and rake λ, using theoretical P-wave radiation pattern polarities (Aki and Richards, 2002) to correct the polarities of P arrivals across the array. The final focal mechanism is chosen as the angle combination that yields the maximum stacked signal S (Equation (3)).

ANALYSIS AND RESULTS

There are serval ways to location and estimate focal mechanism from an earthquake. To achieve automated earthquake location and determination of focal mechanisms of small events from dense-array data, in this study, we demonstrate the success of use both equations introduced above. First, we apply equation (1) to relocate epicenter by stack seismic array waveforms. We selected the 2020 Shilin, Taiwan earthquake as example. The epicentral area of this earthquake is densely covered by seismic stations, and the collected seismic section indicates that the epicentral distance is distributed nearly directly above the source (Figure 1a and b). The source and station configuration is shown in Figure 1b. P-wave polarization data shows that observation points surround the source location, forming four clusters of polarities. Through the relocation analysis conducted in this study, the results indicate that the relocated source coincides to the catalog reported epicenter position from the Central Weather Administration Seismic Network (CWASN), with a depth of 2 kilometers, as shown in Figure 2.

To demonstrate the feasibility of automatically determining focal mechanisms from array seismic waveforms without picking arrival times and polarization directions, this study constructs a computational workflow based on the relation in Equation (3) and extend the polarities as seismic waveforms. First, a set of near-source seismic array waveforms is synthetically generated, as shown in Figure 3a. The source–station distribution represented by these waveforms is shown in Figure 3b. The synthetically generated P-wave polarization shows also as references. Based on waveform stacking procedure, we search the optimum source parameters of azimuth angle, dip angle, and slip angle to find the peak *S* value of equation (3). The final determined source parameters have been used to plot the focal mechanism as shown in Figure 3c with P-wave polarizations. It indicated the well fit for the P-wave polarizations and represented the original source parameters to generate the synthetic waveforms (Figure 3a).

DISCUSSION AND CONCLUSION

Our approach effectively utilizes waveform stacking techniques to improve event localization and focal mechanism estimation. The findings will contribute to a deeper understanding of earthquake triggering processes near a geothermal testing site and have the potential to enhance seismic monitoring strategies for future geothermal power plan operation.

Taiwan has been actively promoting deep geothermal development, with multiple geothermal potential areas identified and specific geothermal sites selected for geophysical exploration, exploratory drilling, and power plant design. Since these sites are in different geological structural zones, the disaster prevention requirements for power plant facilities and the environmental impacts of plant operations vary. However, all sites may be affected by significant nearby natural earthquakes, and induce earthquakes triggered by water reinjection during the operation of geothermal power plants. These factors underscore the importance of seismic monitoring in geothermal areas.

The Ilan plain of Taiwan has been considered as a potential region to further test and building a series of Geothermal power plans. For the special case to evaluate and monitor the Geothermal site located at Ilan during its drilling and operation stages, we should apply above methods to fast report nearby earthquake activity for early warning and decision making. Currently, we presented the examples of earthquake recorded by the regional network which can be equivalent as a small-scale Geothermal drilling site with dense array. Following our works, we will improve our analysis and approach to fit special cases of small-scale Geothermal drilling site. In the future, geothermal monitoring in Taiwan will be equipped with downhole seismic arrays in geothermal wells. Following this report, we will plan to design a seismic array layout and synthetic testing for performance of earthquake monitoring in the coming days before the meeting. Furthermore, we may select various combination to optimum design seismic array for potential specific sites in Taiwan.

Acknowledgements

This study was supported by Academia Sinica, under grant AS-TP-110-M02, the Central Weather Administration, under grant MOTC-CWA-113-E-02, the National Science and Technology Council, Taiwan, under grant NSTC 111-2116-M-001-011.

REFERENCES

Aki, K. and Richards, P. G.: Quantitative Seismology, University Science Books, (2002).

Ishii, M., Shearer, P. M., Houston, H. and Vidale, J. E.: Teleseismic P wave imaging of the 26 December 2004 Sumatra-Andaman and 28 March 2005 Sumatra earthquake ruptures using the Hi-net array, J. Geophys. Res., 122, B11307, doi:10.1029/2006JB004700, (2007).

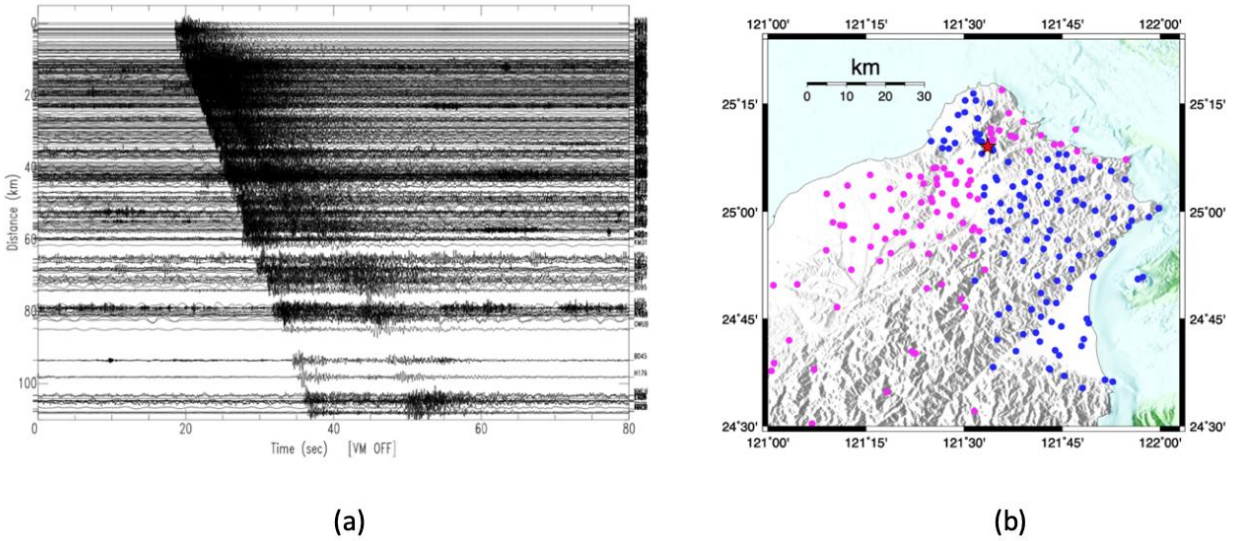


Figure 1. (a). Distance-time section of the collected vertical waveforms for the 2020 Shilin, Taiwan earthquake. The records are filtered through a 0.1 Hz to 5 Hz bandpass filter. Station names are annotated on the right side of the figure. (b). Spatial distribution of seismic stations which recorded seismic waveforms to form above seismic section (Figure 1a). Blue circle symbols represent upward polarity, and purple circle symbols represent downward polarity of the P-wave first-motion.

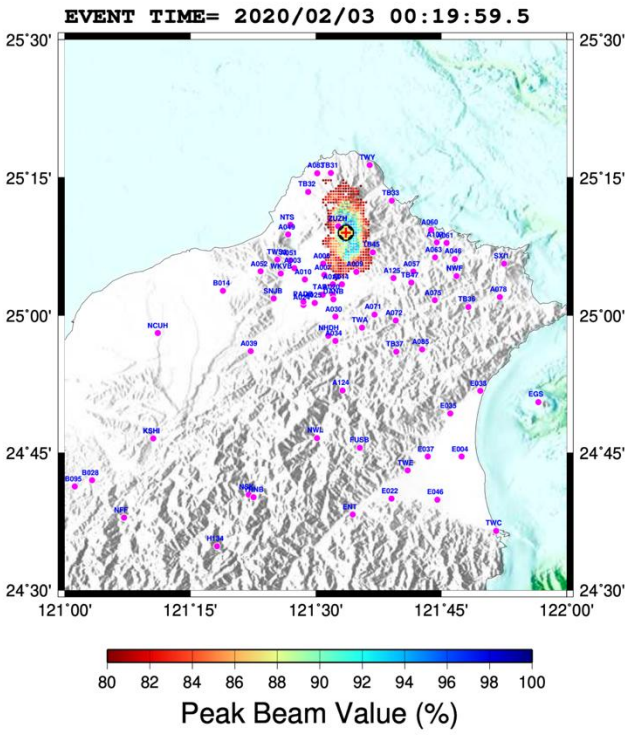
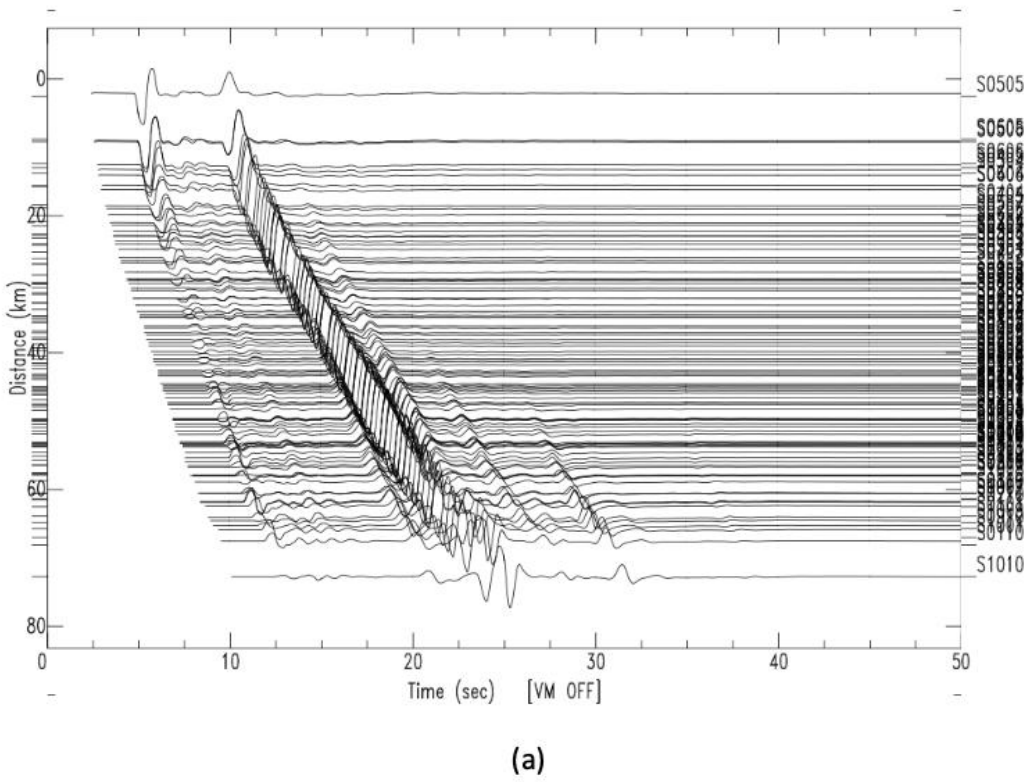
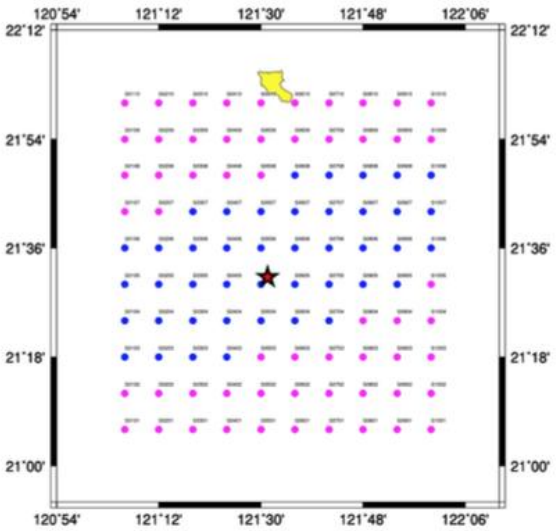


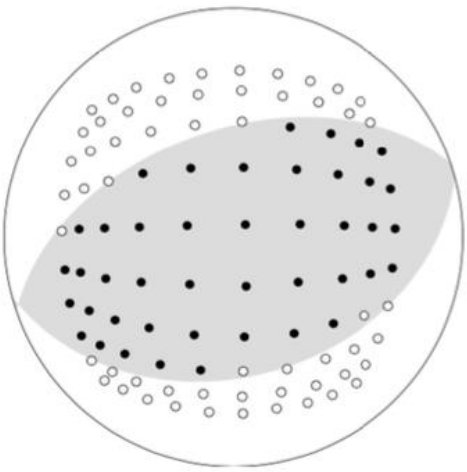
Figure 2. Earthquake relocation based on seismic wave stacking through the backward projection method using only vertical acceleration waveforms of the 2020 Shilin earthquake collected data (Figure 1a). The red cross symbol indicated the epicenter located by this study (source depth of 2.0 km), and gray circle symbol indicated the CWASN located epicenter (source depth of 5.1 km). The distribution of stacking energy and scale bar are shown as depicted. Purple small circle denotes station of waveform selected for stacking and its station name as blue text on top. The estimated event original time is listed in the top of this Figure.



(a)



(b)



(c)

Figure 3. (a). Distance-time section of the synthetic seismic waveforms from a designed seismic array with an earthquake inside the seismic array as shown in Figure 3b. This event is considered as source depth of 30 km, with focal mechanism (strike 60°, dip 45° and slip 90°). (b). Spatial distribution of seismic stations (circles) and the epicenter of earthquake (symbol of red star) which recorded seismic waveforms to form the seismic section (Figure 3a). P-wave polarizations from synthetic modeling are shown in Figure 3b also. Blue circle symbols represent upward polarity, and purple circle symbols represent downward polarity of the P-wave first-motion. (c). The final determined source mechanism plot with P-wave polarizations from synthetics.